Spontaneous Breakdown of Translational Symmetry in Quantum Hall Systems: Crystalline Order in High Landau Levels

F. D. M. Haldane,[1] E. H. Rezayi,[2] and Kun Yang[3]

[1]*Department of Physics, Princeton University, Princeton, New Jersey 08544*

[2]*Department of Physics, California State University, Los Angeles, California 90032*

[3]*National High Magnetic Field Laboratory and Department of Physics, Florida State University, Tallahassee, Florida 32306*

(Received 18 February 2000)

We report on results of systematic numerical studies of two-dimensional electron gas systems subject to a perpendicular magnetic field, with a high Landau level partially filled by electrons. Our results are strongly suggestive of a breakdown of translational symmetry and the presence of crystalline order in the ground state. This is in sharp contrast with the physics of the lowest and first excited Landau levels, and in good qualitative agreement with earlier Hartree-Fock studies. Experimental implications of our results are discussed.

PACS numbers: 73.20.Dx, 73.40.Kp, 73.50.Jt

Recently there has been considerable interest in the behavior of a two-dimensional (2D) electron gas subject to a perpendicular magnetic field, when a high Landau level (LL) (with LL index $N \geq 2$) is partially filled by electrons. This is largely inspired by the recent experimental discovery [1–3] that the transport properties of the system are highly anisotropic and nonlinear for LL filling fraction $\nu = \frac{9}{2}, \frac{11}{2}, \frac{13}{2}, \ldots$. Previously, Hartree-Fock [4–6] (HF) and variational studies [7] suggested that, unlike the $N = 0$ and $N = 1$ LL's [in which either incompressible fractional quantum Hall (FQH) or compressible Fermi-liquid-like states are realized], in $N \geq 2$ LL's the electrons form charge density waves (CDW). In particular, at half-integral filling CDW's break translational symmetry only in one direction and form stripes. Anisotropic transport would indeed result from such a striped (or related) structure [8–11].

We neglect LL mixing, and consider the case where the LL with index N has partial filling $\tilde{\nu}$, while LL's with lower index are completely filled ($\nu = 2N + \tilde{\nu}$). By particle-hole symmetry of the partially filled LL, this is equivalent to $\nu = 2N + 2 - \tilde{\nu}$. We also assume that the partially filled LL is maximally spin polarized at the $\tilde{\nu}$ we consider. Previously [12], we studied such $N \geq 2$ LL's with $\tilde{\nu} = \frac{1}{2}$ by numerically diagonalizing the Hamiltonians of finite-size systems; those results strongly supported the existence of stripe order.

An outstanding issue is the nature of the ground state at high LL's for fillings sufficiently far from the half-filled level. Koulakov, Fogler, and Shklovskii [4,5] (see also Moessner and Chalker [6]) predicted a novel crystalline phase called the "bubble" phase with more than one electron per unit cell outside of the range $\tilde{\nu} = 0.4$–0.6. The bubble crystal has lower energy than the Laughlin state for $\nu = 4 + \frac{1}{3}$ [7]. Experimentally, a reentrant quantum Hall state is found near $\nu = 4 + \frac{1}{4}$ which is quantized as a $\nu = 4$ LL plateau [1–3]. Evidently the electrons in the topmost LL are frozen out of the transport. Pinning of a crystalline structure provides a natural explanation of the reentrant phase and would further explain the observed threshold in conduction [3]. However, this is not entirely conclusive, and other mechanisms for the conduction threshold are also possible [3].

In this paper, we report on new numerical results on systems *away* from half-filling using the unscreened Coulomb interactions. Remarkably, our results suggest that CDW's are formed at all filling factors we have studied, including those that would support prominent FQH states or composite fermion Fermi-liquid states in the lowest or first excited Landau levels. These CDW's, however, have 2D structures and are no longer stripes when the filling factors are sufficiently far away from $\frac{1}{2}$. They are not Wigner crystals [13] either, unless $\tilde{\nu}$ is small (below 0.2). In the intermediate filling factor range, we find each unit cell of the CDW contains more than one electron. Our results are in good agreement with the predicted bubble phase and are the first exact finite-size calculations which exhibit a crystalline state in a system with continuous translational symmetry.

We restrict the states of the electrons to a given LL, and work with periodic boundary conditions (PBC, torus geometry) as in our previous paper [12]. We also set the magnetic length to unity. To detect intrinsically preferred configurations we consider a rectangular PBC unit cell and vary its aspect ratio. The PBC plays a crucial role in removing continuous rotational symmetry, and selecting a discrete set of possible crystal orientations.

In Fig. 1 we plot the energy levels of systems with $N_e = 8$ electrons in the $N = 2$ LL at filling factor $\tilde{\nu} = \frac{1}{4}$ as a function of the aspect ratio. We also show the levels of a system with a hexagonal PBC unit cell at the right side of Fig. 1. A generic feature of the spectra is the existence of a large number of low-lying states whose energies are almost degenerate, which we call the ground state manifold. The momenta of these quasidegenerate states for rectangular geometry with aspect ratio asp = 0.77 and hexagonal

 0031-9007/00/85(25)/5396(4)$15.00

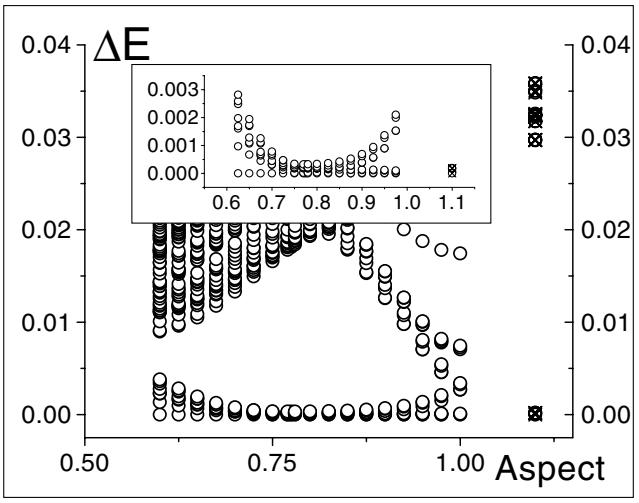

FIG. 1. Energy levels versus aspect ratio for quarter-filled $N = 2$ Landau level with eight electrons and rectangular geometry. The inset is a blowup of the low-energy spectra for aspect ratio between 0.6 and 1.0. The points at 1.1 (open circle plus x) correspond to hexagonal unit cell.

geometry are shown in Fig. 2; they form a 2D superlattice structure, which for the rectangular geometry have the supercell vectors $\mathbf{b}_1 = 2a\hat{e}_x - b\hat{e}_y$ and $\mathbf{b}_2 = 2b\hat{e}_y$, where $a = 2\pi/L_1$ and $b = 2\pi/L_2$. L_1 and L_2 are the dimensions of the unit cell ($L_1 \times L_2 = 2\pi N_\Phi$, N_Φ is the total flux quanta in the system). The area per wave vector in the Brillouin zone (BZ) is $ab = (2\pi)^2/A$, where A is the (real space) area of the system.

There are similarities as well as important differences between these spectra and those of half-filled high LL's [12] with stripe order. As in the stripe case [12], the large quasidegeneracy of the ground state manifold is an indication of broken translational symmetry [14]. The difference here is that (i) the degeneracy is much larger and (ii) the momenta of the low-lying states form 2D instead of 1D arrays. These new features indicate that the translational symmetry is broken in both directions and the ground state is a 2D CDW. In the stripe state, on the other hand, the translational symmetry is broken only in the direction perpendicular to the stripes. Therefore the degeneracy is smaller and the momenta of the low-lying states form a 1D array.

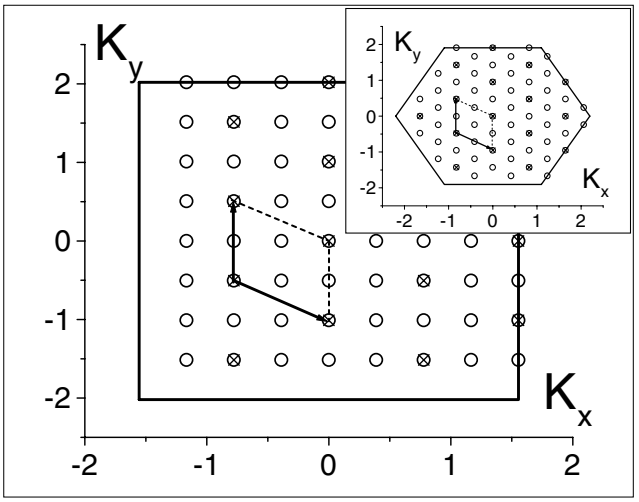

FIG. 2. The allowed (circles) and the ground state manifold momenta (×'s). The data are for a rectangular geometry with asp = 0.77, 8 electrons in the $N = 2$ LL, and $\tilde{\nu} = \frac{1}{4}$. The solid line is the boundary of the Brillouin zone (BZ). The superlattice reciprocal basis vectors are shown by solid arrows. The inset gives the corresponding results for an hexagonal unit cell.

The momenta of the states in the ground state manifold are the reciprocal lattice vectors of the bubble crystal. Transforming to the direct lattice vectors, we obtain $\mathbf{a}_1 = \pi/a\hat{e}_x$ and $\mathbf{a}_2 = \pi/2a\hat{e}_x + \pi/b\hat{e}_y$. For the optimum system, with asp = 0.77, we obtain $a_1 = 8.08$, $a_2 = 7.42$, and $\phi = 57°$. This is very close to a triangular lattice. In the case of the hexagonal PBC unit cell, both the reciprocal superlattice and its direct lattice are triangular.

The number N_D of distinct quasidegenerate ground states allows the number N_b of bubbles in the system, and hence the number $M = N_e/N_b$ of electrons per bubble, to be immediately obtained through the relation $N_b N_D = \bar{N}^2$, where $\bar{N}$ is the highest common divisor of N_e and N_Φ. In our case, $\bar{N} = N_e = 8$, and $N_D = 16$, which gives $N_b = 4$ and $M = 2$ [15]. The Wigner crystal would correspond to $N_b = N_e$ and $M = 1$. In general [16], there are $\bar{N}^2$ distinct values of the total momentum quantum number, which define a BZ of area $(2\pi\bar{N})^2/A$. If translational symmetry is broken, the area of the BZ of the superlattice is then $(2\pi\bar{N})^2/AN_D$, which must be $(2\pi)^2/(A/N_b)$, where A/N_b is the area per bubble; hence $N_b N_D = \bar{N}^2$.

We next turn to the density response functions. In Fig. 3 we show the projected ground state charge susceptibility [12] $\chi(\mathbf{q})$ of one of the optimum rectangular and hexagonal systems described above. The calculation takes into account the contributions from the two lowest energy states in each symmetry subspace; this is an excellent approximation in view of the fact that the response function is dominated by low-energy states because of the energy denominator. We note that $\chi(\mathbf{q})$ exhibits a strong response at the reciprocal lattice vectors (Bragg condition); the background at other wave vectors (shown by ×'s in Fig. 3) are negligible compared to these responses. The origin of the strong response lies in the approximate degeneracy amoung the states forming the ground state manifold. The system responds very strongly to a potential modulation with a wave vector that connects the ground state to one of the low-lying states (which must be a reciprocal lattice vector) because of the small energy denominator. This is also another reason why there must be one low-lying state for each reciprocal lattice vector. A second notable feature is the almost *hexagonal* symmetry of the response, despite the fact that the PBC geometry used in this case was *rectangular.* This indicates that the bubbles tend to form a

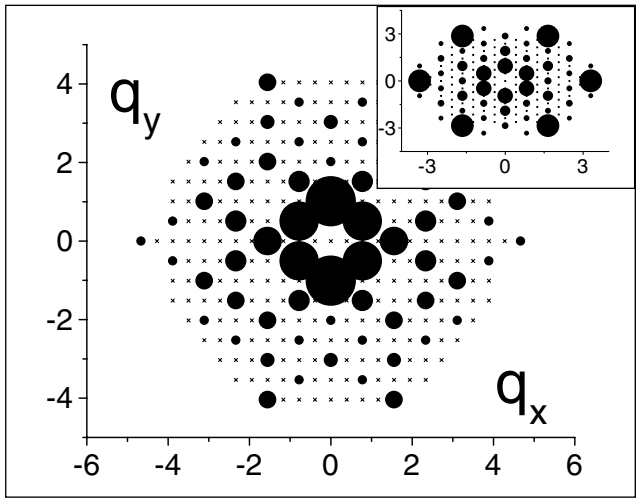

FIG. 3. A 2D plot of the peaks of the projected (or guiding center) charge susceptibility $\chi(\mathbf{q})$ at reciprocal lattice vectors, for a system with $N_e = 8$ at $\tilde{\nu} = \frac{1}{4}$, rectangular geometry with $a = 0.77$. The size of the circles give an indication of the height of the peak at that point. Only responses above 100 have been plotted as solid circles. The zone boundaries are not within the range of the figure. The largest circle corresponds to 16 491. The inset gives the results for a hexagonal unit cell. The $\times$'s are the allowed wave vectors.

triangular lattice, in agreement with the predictions of HF theory.

The tendency toward forming a triangular lattice is also seen in the "guiding center (GC) static structure factor" $S_0(\mathbf{q})$ [12], which we present as a 3D plot in Fig. 4. Here we see sharp peaks with an approximate sixfold symmetry at the primary reciprocal lattice vectors, indicating the presence of strong density correlation at these wave vectors in the ground state.

In Figs. 5 and 6 we plot ground state "projected density" correlation functions in *real* space. These describe correlations relative to the GC (*not* the coordinate) of a particle. The first is the Fourier transform (FT) of

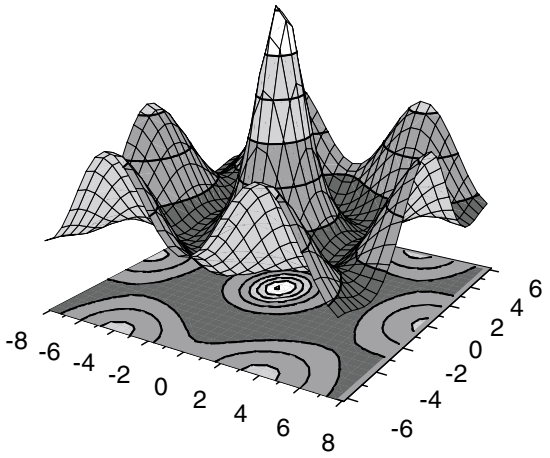

FIG. 5. Real-space "projected density" (guiding center) correlation function, derived from Fig. 4. A 2D contour plot is also included below the 3D plot.

$S_0(\mathbf{q})\exp(-q^2/2)$, which is the electron density of an equivalent lowest-LL system, and gives information on the spatial distribution of GC's. The second is the FT of $S_0(\mathbf{q})[L_N(q^2/2)]^2\exp(-q^2/2)$ with $N = 2$ (L_N is a Laguerre polynomial): this (plus the uniform density of the filled LL's) represents the actual electron density.

In Fig. 5 the presence of four bubbles and the relative orientation of the bubbles can be clearly seen, and there is strong crystalline order of the GC distribution. The central peak contains two electrons, one of which is the particle with the GC at the origin. For $N > 0$, as in Fig. 6, only weak order is displayed by the actual electron density, because of the averaging effect of the cyclotron motion around the GC's. It is the *guiding centers* of the electrons that form bubbles as anticipated in Ref. [7] (Fig. 1). The electrons themselves manage to stay apart to lower the Coulomb repulsion, in spite of the clustering of their GC's.

We have also explored other filling factors in the $N = 2$ LL such as $\tilde{\nu} = \frac{2}{5}$ and $\tilde{\nu} = \frac{1}{3}$, where the system would

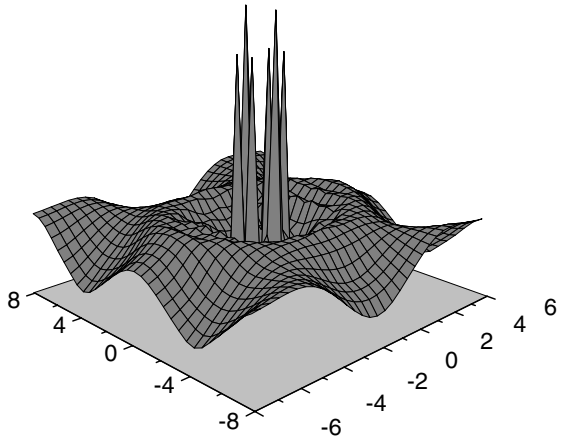

FIG. 4. A 3D plot of the guiding center structure factor $S_0(\mathbf{q})$ (same system as Fig. 3). The signature of the hexagonal lattice is seen in the near sixfold symmetry of the peaks.

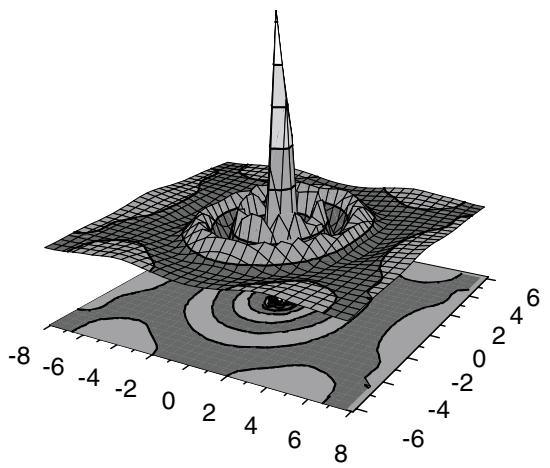

FIG. 6. $N = 2$ Landau level full electron density correlations (relative to a guiding center), derived from Fig. 4.

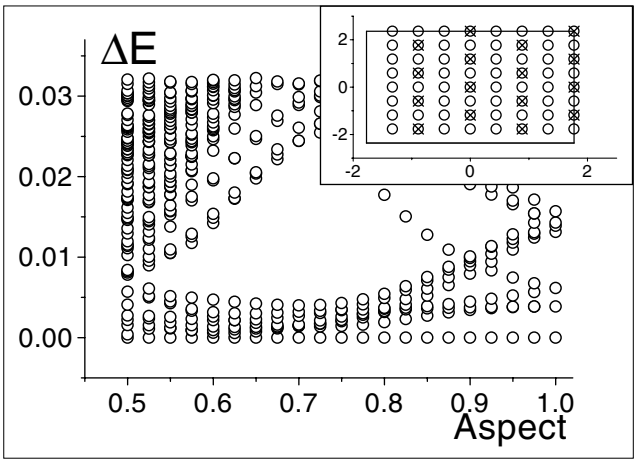

FIG. 7. Spectra of systems with eight electrons at $\tilde{\nu} = \frac{1}{3}$ in the $N = 2$ LL, with rectangular geometry and various aspect ratios. The inset plots the momenta of the low-lying states for asp = 0.75, in the same was as Fig. 2.

condense into prominent FQH states if it was in the lowest LL; here, however, our studies suggest formation of CDW's instead. For $\tilde{\nu} = \frac{1}{3}$ we obtain similar behavior to $\tilde{\nu} = \frac{1}{4}$: the energy spectra as a function of the aspect ratio shown in Fig. 7 is very similar to Fig. 1 and indicates formation of a 2D CDW. Using the degeneracy of the ground state manifold, we find the number of electrons per bubble is also two. The energies of the states in the ground state manifold, however, are not as close as the $\tilde{\nu} = \frac{1}{4}$. This results in weaker peaks in $\chi(\mathbf{q})$ at the reciprocal lattice vectors.

We interpret this to be an indication that, in this LL, $\tilde{\nu} = \frac{1}{4}$ is more favorable than $\tilde{\nu} = \frac{1}{3}$ for formation of a two-electron bubble phase. In real systems a crystal is always pinned by a disorder potential, and in a nonlinear transport measurement, there should be a threshold depinning field at which there is a sharp feature in the I-V curve. A weaker crystal would result in a more diffuse conduction threshold as various portions of the crystal get depinned at different current values, while a stronger one, on the other hand, will have sharp conduction threshold. This is consistent with the observation of Cooper *et al.* [3] that there is a sharp threshold region at about $\tilde{\nu} = \frac{1}{4}$, but more diffuse thresholds at both higher and lower $\tilde{\nu}$.

In contrast to $\tilde{\nu} = \frac{1}{4}$ and $\tilde{\nu} = \frac{1}{3}$, the spectra for $\tilde{\nu} = \frac{2}{5}$ was found to be very similar to $\tilde{\nu} = \frac{1}{2}$ [12]. The momenta of the low-lying states belong to a 1D array, indicating formation of a 1D CDW or stripe phase; the weight of the HF state 11110000001111000000 ($N_e = 8$), in a rectangular geometry with an aspect ratio of 0.80, is about 65%. We conclude that the transition from stripe to bubble phases occurs between $\tilde{\nu} = \frac{1}{3}$ and $\tilde{\nu} = \frac{2}{5}$, in qualitative agreement with HF predictions [5,6]. We have also studied higher LL's. The results are similar and will be reported elsewhere.

We have benefited from stimulating discussions with J. P. Eisenstein, K. B. Cooper, and M. P. Lilly. We thank B. I. Shklovskii and M. M. Fogler for helpful comments. This work was supported by NSF DMR-9420560 and DMR-0086191 (E. H. R.), DMR-9809483 (F. D. M. H.), DMR-9971541, and the Sloan Foundation (K. Y.). E. H. R. acknowledges the hospitality of ITP Santa Barbara, supported by NSF-PHY94-07194, where part of the work was performed.

[1] M. P. Lilly, K. B. Cooper, J. P. Eisenstein, L. N. Pfeiffer, and K. W. West, Phys. Rev. Lett. **82**, 394 (1999).
[2] R. R. Du, D. C. Tsui, H. L. Stormer, L. N. Pfeiffer, K. W. Baldwin, and K. W. West, Solid State Commun. **109**, 389 (1999).
[3] K. B. Cooper, M. P. Lilly, J. P. Eisenstein, L. N. Pfeiffer, and K. W. West, Phys. Rev. B **60**, R11 285 (1999).
[4] A. A. Koulakov, M. M. Fogler, and B. I. Shklovskii, Phys. Rev. Lett. **76**, 499 (1996).
[5] M. M. Fogler, A. A. Koulakov, and B. I. Shklovskii, Phys. Rev. B **54**, 1853 (1996).
[6] R. Moessner and J. T. Chalker, Phys. Rev. B **54**, 5006 (1996).
[7] M. M. Fogler and A. A. Koulakov, Phys. Rev. B **55**, 9326 (1997).
[8] E. Fradkin and S. A. Kivelson, Phys. Rev. B **59**, 8065 (1999); E. Fradkin, S. A. Kivelson, E. Manousakis, and K. Nho, Phys. Rev. Lett. **84,** 1982 (2000).
[9] H. A. Fertig, Phys. Rev. Lett. **82**, 3693 (1999).
[10] A. H. MacDonald and M. P. A. Fisher, Phys. Rev. B **61**, 5724 (2000).
[11] T. Stanescu, I. Martin, and P. Phillips, Phys. Rev. Lett. **84**, 1288 (2000).
[12] E. H. Rezayi, F. D. M. Haldane, and K. Yang, Phys. Rev. Lett. **83**, 1219 (1999).
[13] H. Fukuyama, P. M. Platzman, and P. W. Anderson, Phys. Rev. B **19**, 5211 (1979).
[14] True broken translational symmetry with exact ground state degeneracy occurs only in the infinite-size limit; at finite size, this becomes a quasidegeneracy.
[15] This result is in overall agreement with the estimate of Ref. [5]: $M = 3\tilde{\nu}N$.
[16] F. D. M. Haldane, Phys. Rev. Lett. **55**, 2095 (1985).